Thesis for the degree of Master of Philosophy

Carbon Nanotube-Graphene Nanoplatelet Hybrids and their Composites in Polymeric Binders of Lithium-ion Negative electrode

The Graduate School of University of Ulsan
School of Chemical Engineering

SUGARTSEREN NYAMBAYAR

Carbon nanotube-graphene nanoplatelet hybrids and their polymer composites as binders for lithium-ion Negative electrode

Supervisor: Professor Eun-Suok Oh

A Dissertation

Submitted to
The Graduate School of the University of Ulsan
In partial Fulfillment of the Requirements
For the Degree of

Master

by

Sugartseren Nyambayar

School of Chemical Engineering
University of Ulsan, Korea
February 2019

Carbon Nanotube-Graphene Nanoplatelet Hybrids and their Composites in Polymeric Binders of Lithium-ion Negative electrode

This certifies that the master's thesis of Sugartseren Nyambayar is approved.

Committee Chair Prof. Sung Gu Kang

Committee Member Prof. Jun Bom Kim

Committee Member Prof. Won Mook Choi

School of Chemical Engineering

University of Ulsan, Korea

February 2019

ACKNOWLEDGEMENT

To all those people, who had been helped me during my graduate studies.

I would first like to thank my thesis advisor professor Eun-Suok Oh. The door to Prof. Oh office was always open whenever I ran into a trouble spot or had a question about my research or writing. He consistently allowed this paper to be my own work, but steered me in the right the direction whenever he thought I needed it. Always remember our first greetings when I was tried to apply to graduate school. Never regret for choice of Energy Nano Lab and our professor.

Thank you for always try to cheer me by anyway, encouraging my research study, giving me a helpful comments, advices. All of your precious advices and comments have been helped me a lot and in all way. Even though I had hard times during my studies, I have passed it because of your priceless support and encouragement.

Also, this thesis would not be completed unless I had my labmates like family members. Always supported and helped, cheering each other, going through our hard times together. All of your soul and mind without this, any of our research would not be perfect.

A very special thanks to my family, my parents who support me from Mongolia, my daughter and husband supporting and cheering me for all of the sacrifices. Cannot express how I am happy with them and their support they provided me over the years. Their unconditional love for me was my super protector at hardship.

Finally, thanks to my lovely friends who were always by my side, helped me to achieve my goal.

Grateful what I have now and what I will have in the future ☺

Abstract

Graphene nanoplatelet (GnP), which consists of small stack of graphene, is used as a reinforcement to enhance the performance of the poly(acrylonitrile-butyl acrylate) (PANBA) binder in a lithium ion battery (LIB). To the best of our knowledge, this is the first time that a conductive nanofillers such as CNT and GnP has been used in a conventional water-dispersed polymer and applied as a binder for LIB. This study presents a new water-based conductive binder composed of carbon nanotube (CNT) and graphene nanoplatelet (GnP) for graphite and LTO ($Li_4Ti_{15}O_{12}$) negative electrode and graphite electrode. A solution containing a certain amount of CNT, GnP, or both was used to synthesize emulsified poly(acrylonitrile-butyl acrylate) (PANBA) containing conductive CNT, GnP, or CNT_xGnP_{1-x} hybrids. These polymers were applied as binders for the LTO electrodes and compared to the nonconductive PANBA binder with respect to the electrochemical performance and applied for graphite electrodes and compared with commercial 480B binder. The conductive $CNT_xGnP_{1※}$PANBA binders showed several advantages: superior water-dispersion stability and elongation, lower transport resistances for electron and lithium ions, and lower charge transfer resistance. This led to stable cyclic capacity above 130 mAh g^{-1} at the 100^{th} cycle for the $CNT_xGnP_{1※}$PANBA for LTO electrodes without conducting agents and high capacity retention of 5C/0.2C above 58.0 %, whereas the nonconductive PANBA-LTO electrode showed the cyclic capacity of 118 mAh g^{-1} at the 100^{th} cycle and the capacity retention of 5C/0.2C of 44.1%.

Contents

3. Results and discussion

Figure list

Table list

1. Introduction

1.1. Lithium ion batteries

A battery is a collection of one or more cells whose electrochemical reactions create a flow of electrons in a circuit. Most of batteries are consist of three basic components: an anode (negative electrode), a cathode (positive electrode) and some kind of electrolyte (substance that chemically reacts with the negative electrode and positive electrode). Primary batteries must be thrown away after use. However, Secondary batteries can be recharged many times because their electrochemical reaction is reversible. Therefore, it can be discharged and charged many times.

The oldest generation of secondary battery is the lead-acid battery. It was invented by the French physician Gaston Plante in 1859. The grid structure of the lead-acid battery is made from a lead alloy. After this battery, the active components of a rechargeable NiCd battery has been invented. It consist of nickel hydroxide (NiOH) in the positive electrode and cadmium (Cd) in the negative electrode. Due to their low internal resistance and toxicity of cadmium limits the use of NiCd batteries. Times goes by the world has been more and more dependent on rechargeable batteries.

Modern Lithium-ion batteries hold more than twice as much energy by weight that of the standard nickel-cadmium as the first commercial one which sold by Sony 1991. [1–3]Lithium metal is the lightest of all metals and it has greatest electrochemical potential and provides the largest energy density for weight. There are many failures to develop rechargeable lithium batteries due to their safety problems. Because of the essential instability of lithium metal, especially during charging. Lithium ion battery has potential for higher energy densities. The high cell voltage of 3.6 volts allows battery pack with only one cell. Lithium-ion is a low maintenance battery [4–6] which has no memory and no scheduled cycling is required to extend battery's life. In Lithium ion battery, Lithium ion moves from the negative electrode to the positive electrode during discharging and when back charging, and the theoretical lithium storage capacity of the graphite anode has been considered as 372 mAh g^{-1}, corresponding to the first stage of LiC_6. For these compatible reasons, LIB are widely used in power-hungry laptops, cameras, mobile phones and electric cars.

1.2. The components and principle of lithium ion batteries

Lithium ion batteries are made up of four basic components: an anode (negative electrode), a cathode (positive electrode), electrolyte and separator. Both anode and cathode are types of electrodes, these are conductors through which electricity enters or leaves a components in a circuits. Graphite anode materials are used in a broad range of Lithium ion battery manufacturing process, from research laboratories to commercial production plants. Graphite materials offer exceptional first charge efficiency, excellent cost performance ratio and a long life cycle. However nowadays, LTO (Lithium titanate) becomes competing materials with graphite in the anode of a standard lithium-ion battery and the material due to their advantages such as the absence of SEI [7–9] film formation and lithium plating when fast charging at low temperature.

In LIBs, electrolyte is capable of transporting Li^+ ions between the chemical reactions that happen at the negative electrode and positive electrode. Therefore, liquid or gel conducting materials support the Li^+ transporting better than solid materials. Liquid electrolyte in lithium ion battery consist of lithium salt ($LiPF_6$, $LiBF_4$ or $LiClO_4$ so on) in organic solvent mixtures which keep their electrochemical stability within range of the operating voltage and have a high thermal and chemical stability. Separator prevents anode material and cathode material from contacting each other due to cause a short circuit in the battery. If it contact to each other and make electrical short to battery, it can increase battery temperature even can be explode.

A schematic operation of lithium-ion battery is shown in Figure 1.

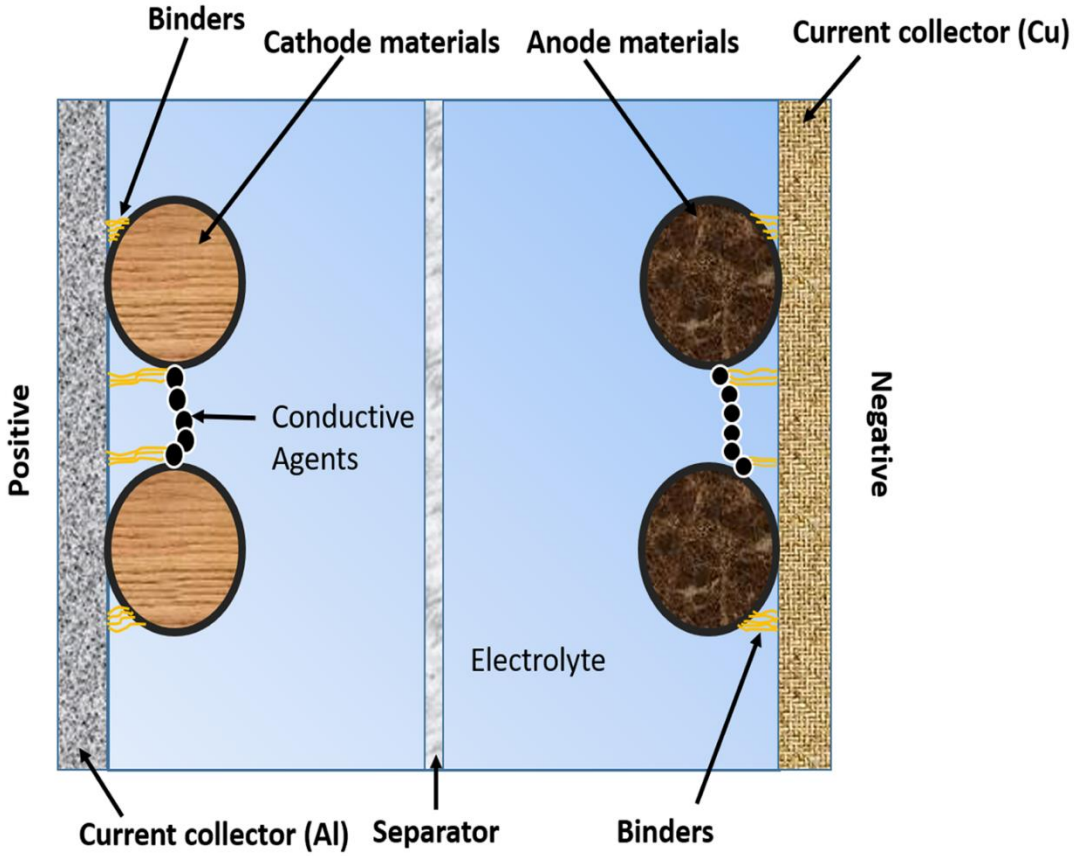

Figure 1. Schematic illustration of Lithium ion battery

1.3. The binder for Lithium ion battery

The binder is one of small part of LIB but it played important role on the electrochemical performance of LIB. Clearly shown in Fig. 2 about how binder material and active material connected on the current collector. Still now, researchers haven't find the binder which is more suitable for preparing transition metal oxides anodes of LIBs. Nowadays, in recent years, binders have been on focus of researchers who work on lithium ion batteries. There are some requirements for good binders of lithium ion battery, shown in Table 1. Therefore, in order to expand the electrochemical performance of lithium ion battery, not only working on to create new electrode materials, importantly find a new electrode processing parts. Generally anode contains 3-5% of binder and it can cover anode and cathode materials. Binders used for making electrode to hold the active material particles together in order to contact with current collector. There are several parameters which binder needed to depend on such as adhesion strength between the electrode and current collector, the interface between the polymers and active particles, interaction of the binder with electrolyte solution, and binder's mechanical characteristics.

Nowadays, increasing of environmental problems battery researchers also need to focus on environmental friendly battery production and disposal. In order to do that, it's important to choose type of binder in the electrode composition to optimize electrode cost, stability of electrode and production procedures. Commercial binders are PVdF (Polyvinylidene fluoride)[4,10,11], SBR (styrene butadiene), CMC (carboxymethyl cellulose)[12–16], and Polyacrylonitrile studied. Except CMC and SBR binders, PVdF commercial binders is dissolved in organic solvent which is N-methyl pyrrolidone (NMP) that needed to purified with additional costs in overall process and not environmental friendly. Also CMC and SBR binders have been shown better performance than PVdF binder in anode materials of lithium ion batteries.

Due to this problem of commercial binder, recent works more focused on water based binders such as CMC and SBR. For processing requirements, cost and environmental issues of binder manufactures, researchers try to less use of PVdF and instead of it use aqueous based binders. Therefore, aqueous binders has some advantages such as lower cost of manufacturing, use water based solvents for environmental problems, higher energy density.

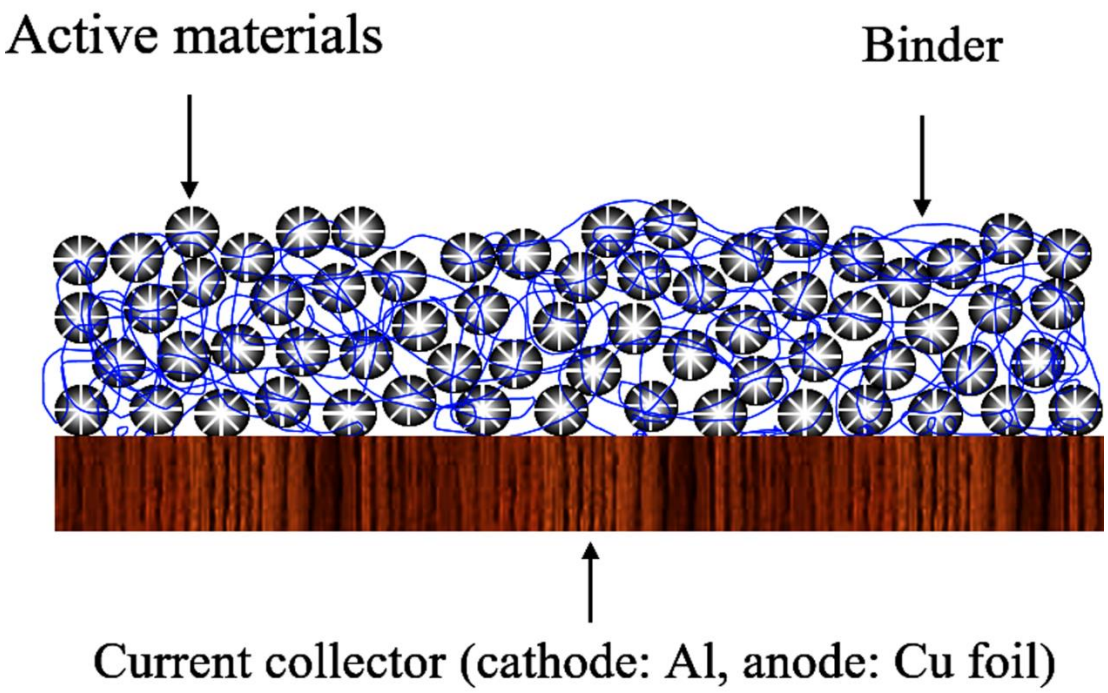

Figure 2. Illustration of connection of active material, binder material on current collector

Table 1. Required characteristics for binders

For battery performance	For productivity
Electrochemical stability over a wide potential range	Viscosity of slurry remains constant over long periods
High melting points	Easily shaped in a roll press without spring back
Good lithium ion and electron conductivity	
Excellent adhesion to electrode	Resistant to chipping during electrode slitting
Good retention of active materials	

1.3.1 Organic-solvent based binder

Organic-solvent based binder means that a binder using organic solvent to dissolve the binder. PVDF is the main example and commercial binder which uses organic solvent for dissolving because it has proper properties to be a LIB binder. During charging and discharging process, PVDF doesn't react with electrolyte and active materials. PVDF repeats the unit of fluorine functional group and during reaction it forms hydrogen bond with surface of active material.

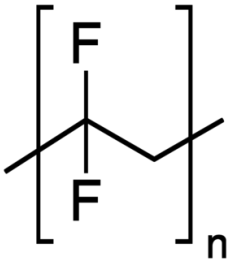

As a result of PVDF, requires organic solvent which is NMP (n-methyl-2-pyrrolidone) as solvent to dissolve PVDF and it afford chemical and electrochemical stability. Additionally, PVDF offers a possibility of high voltage operation during charging and discharging process and not pretend to react with lithium and electrolyte solution. However, glass transition temperature (T_g) of PVdF is about -35˚C and melting temperature is around 177˚C because of this low melting point it can cause a heat stability problems. For example, in commercial graphite electrode, solid electrolyte interface (SEI) breaks down around 120-140˚C and Li_xC_6 start to react with the PVdF[17–19] binder at temperature above 300˚C and then exothermic reaction can be released because of dehydrofluorination of PVdF and to form LiF and hydrogen. In the result of that, released heat and gas generation might damage the cell performance and also some dangerous safety problems (such as exploding) can be appeared. There are more drawbacks around PVdF binders such as it has high irreversible capacity caused by SEI layer and neutral rate of charge and discharge makes replace them by more safety and environmental friendly binders.

1.3.2 Water based binder

In commercial LIB producing process, PVdF is the mostly used in the cathode and anode slurry. Some of drawbacks of PVdF binders, researchers and manufacturers are trying to replace it with binders which has more advantages for environmental and cost issues.[20–23] According to do that, water-based or water-dispersed hybrid binders which use water as a solvent for dissolving binder such as carboxymethyl cellulose (CMC), styrene-butadiene rubber (SBR), poly(acrylonitrile-butyl acrylate) (P(AN-BA)), alginate (a natural polysaccharide extracted from brown algae) and other polymers have gained significant interest in the electrode of LIB manufacturing process and most of water-based binders successfully have been testing these days.

In recent years, researchers have been working on combination of SBR and CMC binder which SBR (styrene-butadiene) as a primary binder and CMC (carboxymethyl cellulose) as a thickening/setting agent. These combination binders can be used in anodes of lithium ion cells, but need more works to process for cathode slurries.

However, water-based binders cannot be used for cathode slurry because most of cathode active materials are metal oxide, therefore, if a small amount of water remained in cathode electrode, it can react with metal atom in cathode and it can be explode or damage the cell.

1.3.3 Objectives

A lot of attentions have been to develop anode materials of lithium ion batteries and applied to electric devices such as cellphone, laptop and also some electric vehicles, and energy storage system etc,. From this interest, we can know that how battery is big part of life and how researchers and developers trying so hard to improve their high performance. In anode materials point of view, there are many candidate of high capacity active materials such as silicon, tin, metal oxide. Interestingly silicon has very high theoretical capacity than other active materials but it has big drawbacks that researchers still working hard to improve it is volume expansion during charge and discharge process. Graphite and lithium titanate (LTO)[24–26] active materials has lower theoretical capacity than silicon but they are stable during charge and discharge process. It makes them to be a main candidates of anode materials of lithium ion battery.

In this study, we have been more focus on binder of anode electrode of lithium battery, but not just binder, binder can disperse in water in Fig. 3 which has good advantage of environmental issue. Using of water-based binder can bring many advantages to lithium ion battery industry, such as non-toxic solvent used, can reduce the manufacturing cost, solving safety issues, no heat stability problems like PVDF binder, high adhesion water-based binder can increase the battery cycle & rate performance. According to that we have made emulsion polymerization to synthesize CNT (carbon nanotube), GnP (Graphene nanoplatelet) with polymer P(AN-BA) to get new hybrid water-based binder to increase the performance of anode material of lithium ion battery.

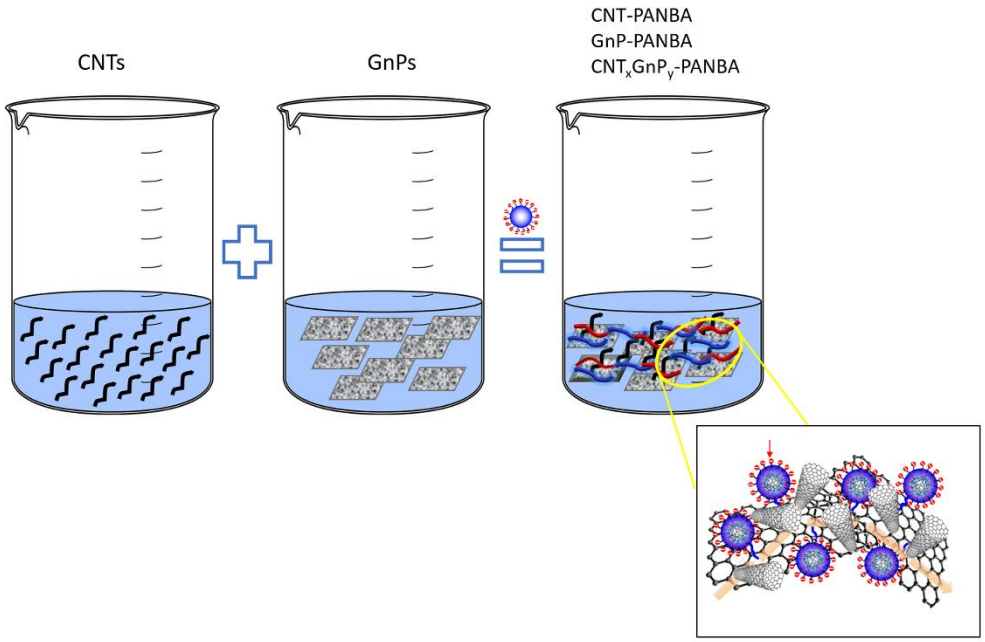

Figure 3. Schematic illustration of CNT and GnP water-based binder.

2. Experimental

2.1. Synthesis of CNT-PANBA, GnP-PANBA by emulsion polymerization

The synthesis of CNT (from China) with polymer, first need to pre-dispersion of CNT 5 wt% paste in distilled water for 4 hours using ice bath sonication. After pre-dispersion of CNT solution, the copolymers of AN and BA(Junsei Chemical Co., Japan) were prepared by emulsion polymerization at 70˚C, follow the batch process. Potassium persulfate (KPS, Sigma-Aldrich) and sodium dodecyl sulfate (SDS, Tokyo Chemical Industry Co.) were used as an initiator and emulsifier, respectively. A pre-dispersed CNT in water solution with different ratio and mixture of AN/BA was examined as monomers for the emulsion polymerization.[12,27] Aqueous CNT solution and mixture of AN/BA were first stirred at room temperature in a four-necked flask equipped with a reflux condenser for 1 h under bubbling nitrogen gas to remove oxygen. A specific amount of KPS (approximately 1 part of the monomer) solution was added to the reactor after increasing the temperature to 70˚C. This step was prolonged for 4hrs to complete the polymerization. The schematic illustration of emulsion polymerization shown in Fig 4. Then the reactor was cooled down to room temperature. GnP(Deokyang Co., Korea) solution with polymer AN/BA synthesized by emulsion polymerization has same process with CNT-PANBA emulsion polymerization. More detailed ratio of samples shown in Table 2.

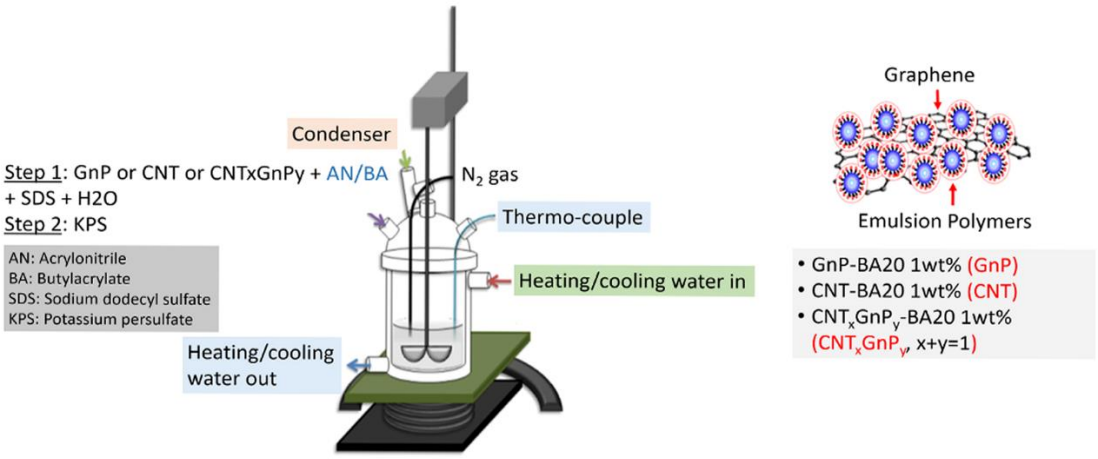

Figure 4. Emulsion polymerization of CNT & GnP-AN/BA

2.2. Synthesis of CNT & GnP with different ratio by emulsion polymerization

A composite mixture of CNT and GnP solution with a mixture of AN/BA was synthesized same method with CNT-PANBA and GnP-PANBA samples by emulsion polymerization. The AN, BA monomers were purchased from Junsei Chemical Co., Ltd., Japan. Commercial grades of potassium persulfate (KPS, Sigma-Aldrich) and sodium dodecyl sulfate (SDS, Tokyo Chemical Industry Co.) were also used as the initiator and emulsifier, respectively, for the polymerization. First of all, composite mixture of CNT and GnP in distilled water solution were initially mixed with the SDS emulsifier and an aqueous mixture of the monomer in a four-necked flask equipped with a reflux condenser under nitrogen gas bubbling at 70˚C for 1hr. Then, a small amount of KPS (approximately one part of the total monomer) dissolved in water was added to the reactor under a nitrogen atmosphere. The polymerization was performed for 4hrs for the completion. More detailed composite mixture ratio of CNT and GnP shown in Table 2.

Table 2. Amounts of monomers used for the emulsion polymerization

	CNT	GnP	AN/BA (g/g)	SDS (g)	KPS (g)
Polymer AN/BA	-	-	10/20	30	10
CNT-PANBA	1	-	10/20	30	10
GnP-PANBA	-	1	10/20	30	10
CG82-PANBA	0.8	0.2	10/20	30	10
CG55-PANBA	0.5	0.5	10/20	30	10

2.3. Electrode preparation and cell assembly

2.3.1. LTO electrode

For the electrochemical tests, the CNT-PANBA, GnP-PANBA, CG82-PANBA, CG55-PANBA were used as water-based binders for LIB anodes, a typical P(AN-BA) binder was considered as a reference binder. The electrode composition was 95 wt% LTO (Posco ESM Co.) as the active material, 2 wt% CMC (Daicel FineChem Ltd., Japan), and 3 wt% synthesized CNT-PANBA, GnP-PANBA, CG82-PANBA and CG55-PANBA. Distilled water was used as a solvent for all cases. After approximately 1hr mixing with planetary ball mill (Pulverisette 7, Fritsch; speed 320 rpm), the slurry was coated to the 20 μm Al-foil by an automatic film coating apparatus. After coating the electrode was dried in convention oven at 60˚C for 30 min, followed by vacuum drying overnight at 70˚C. The loading of the LTO electrode was 3.9 ±0.1 mg/cm^2.

2.3.2. Graphite electrode

CNT-PANBA, GnP-PANBA, CG82-PANBA, CG55-PANBA synthesized binders were used as binder of electrode, and a typical 480B binder was considered as a reference binder. Electrode composition was 90 wt% artificial graphite (SCMG-AR, Showa denko, Japan) as an active material, vapor grown carbon fiber (VGCF, 2 wt%) as a conductive material, CMC binder (3 wt%), and synthesized binder (5 wt%). Distilled water was used as a solvent for all cases. Slurry mixed by homogenizer (Ace Homogenizer, Nihoenseiki Kaishi Ltd., Japan) for 1hr. The mixed slurry were coated on the 18-μm-thick Cu foil shown in Fig 5 and dried in a convection oven at 60˚C for 30min and in a vacuum oven at 70˚C for a day to completely remove the remaining solvent before cell assembly. The loading of the graphite electrode was 4.2±0.2 g/cm^2.

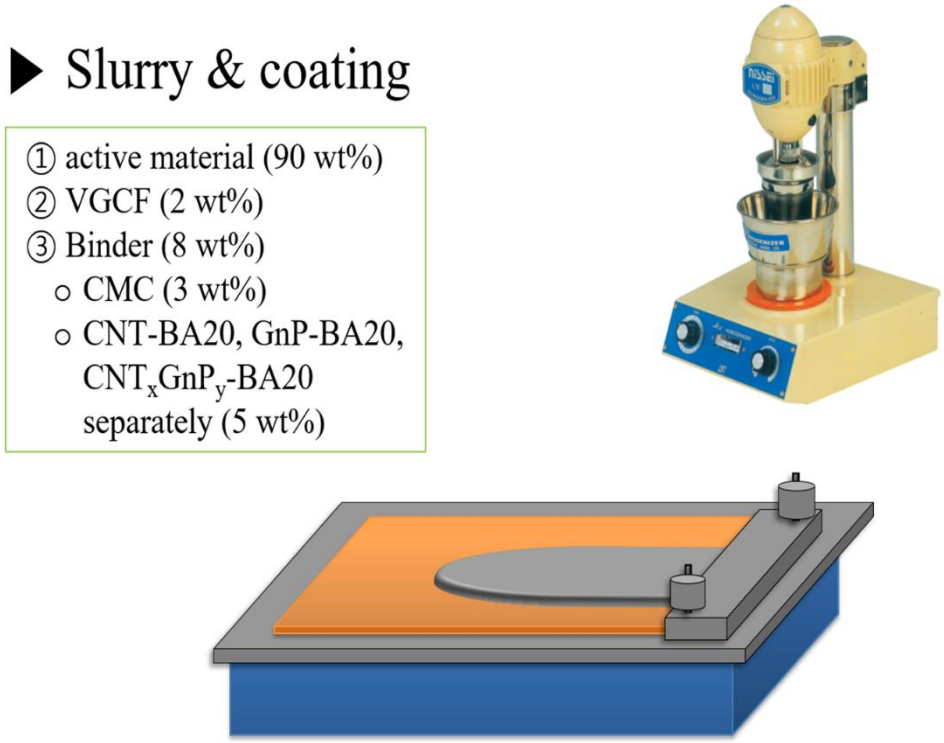

Figure 5. The process of graphite electrode preparation

2.3.3. Cell assembly

The electrodes after dried in vacuum oven were punched by diameter of 14 mm, and cell assembled in an argon-filled glove box. 1M $LiPF_6$ in 1:1:1 ethylene carbonate (EC) : dimethyl carbonate (DMC) : ethyl methyl carbonate (EMC) (Panaxetec Co., Korea) by volume was used as an electrolyte to produce the CR2032 type coin-half cell. The LTO and graphite electrode in both case they assembled with lithium metal as a counter electrode.

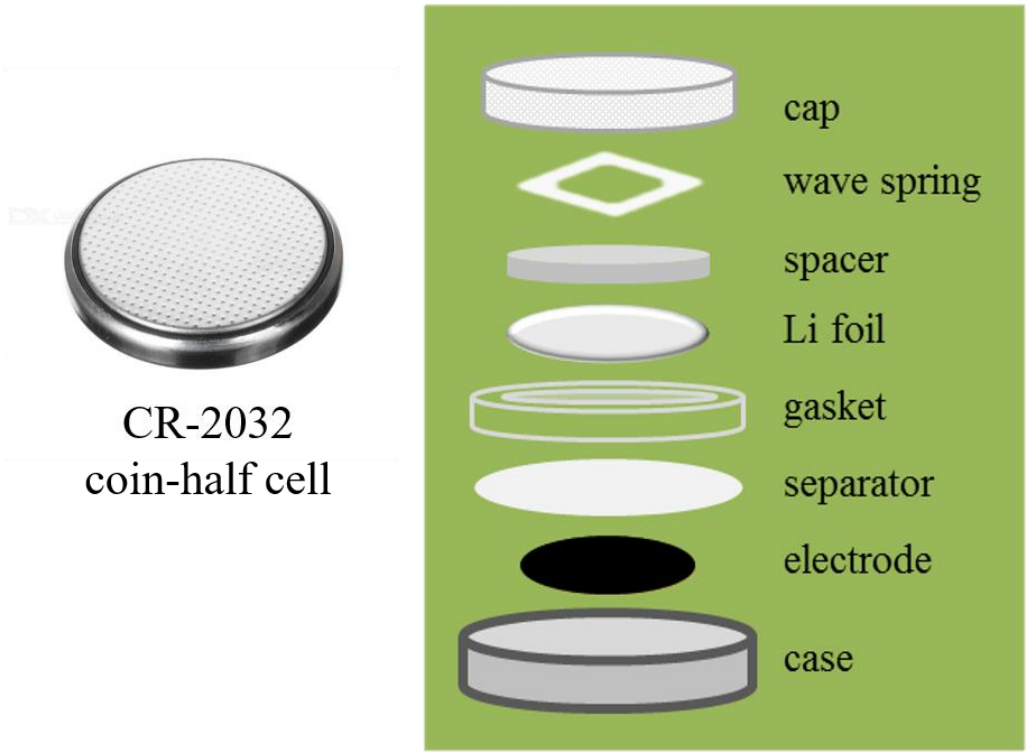

Figure 6. Cell assembly of Lithium ion battery

2.4 Binder characterization

2.4.1. Thermogravimetric Analysis

Thermogravimetric Analyses (TGA) were performed using aluminum pans in order to characterize the binder's thermal stability (Q50 TA Instrument). The binders were first dried for an overnight at 70˚C and then heated at 10˚C/min up to 800˚C in nitrogen atmosphere.

2.4.2. Fourier-Tranform Infrared Spectroscopy

An infrared spectrum represents a fingerprint of a sample with absorption peaks which correspond to the frequencies of vibrations between the bonds of the atoms making up the material. CNT-PANBA, GnP-PANBA, CG82-PANBA, CG55-PANBA were analyzed by fourier transform infrared (FT-IR, Nicolet IR 200, Thermo Scientific) spectra from 600 c m-1 for analyzing material characterization. The FT-IR was conducted by using potassium bromide pellets.

2.4.3. Contact angle

The polymeric binder was coated on Al foil and dried in a convection oven at 60˚C for 30 min and in a vacuum oven at 70˚C overnight to become an approximately 1.2 μm-thick binder film. A specimen of diameter of 14 mm cut and attached on a glass substrate by double-sided tape to avoid any displacement. By contact angle measurement, we can measure function of time exposed to an electrolyte droplet on the binder films using a video-connected device (Theta Lite 100, KSV Instrument Ltd., Finland) in order to investigate the wettability of the binder film.

2.4.4. Elongation Test

A texture analyzer (TA-Plus, Lloyd Instruments Ltd.,) was used to determine the Young modulus of the binders by measuring the tear and peel test. Before test, binders dried for an overnight at 70˚C in the convection oven. Sample preparation is to cut the samples into rectangle shape size of 4 c m x 1 c m. Thickness of the prepared samples should be around 23~25 μm. Peeling force (50N) was controlled from the software.

2.4.5 Sheet Resistance

The conductivities were measured by using sheet resistance (CMT-100MP, AIT Co., Ltd.) with four probe method at 1.5V. The sample preparation was that dried binder film on Aluminum dish at 60˚C in convection oven for overnight, then peel off the dried binder film from Al dish and punched into circle shape, diameter of circle is 14mm.

2.5. Electrode characterization

2.5.1 Adhesion strength

A texture analyzer (TA-PLUS, Lloyd Instruments Ltd.,) was used to measure adhesion strength of graphite electrode by measuring 180˚ peel strength of the electrode strips (20 mm width). A double-sided tape was applied into a stainless steel substrate and an auto adhesive machine was used to adhere the electrode strip carefully. Samples were done setting by vertically to the bottom vise. Cu foil was peeled off using the top sample vise at the direction of 180˚ angle and the force was recorded during experiment.

2.5.2 Electrochemical properties

The electrochemical impedance spectroscopy (EIS, VSP, Biologic Science Instruments) test was operated over a frequency range of 100 kHz to 0.01 Hz. LTO electrode were measured at 1.55V. Graphite electrode were measured at 0V. The cells were charged and discharged over voltage range of 1 to 2.6V in battery cycler (PNE solution Co., Korea) with a 0.1C rate for the first 2 cycles and a 1C rate for the next 100 cycles. The rate capability of the electrode was also tested at various charge/discharge current rates.

3. Results and discussion

3.1 Binder characterization

FT-IR characterization was performed to confirm the chemical bonding between Acrylonitrile-butylacrylate and composite nanofiller's of CNT and GnPs. The results are shown in Figure 7. The FT-IR spectrum of PANBA and hybrid nanofillers of CNT-, GnP- and their composites shows a sharp peak at ~1782 cm^{-1}, which represents the ester group (-C=O) of acrylonitrile-co-butylacrylate. Also at ~2240 cm^{-1}, there is cyano group (-C≡N) of polymer binder. Therefore, graphite and LTO electrode chosen to clearly see the effect of nonconductive PANBA binder and conductive CNT-, GnP-, and CNT_xGnP_y hybrid binders because it has lower transport resistances for electron and lithium ions.

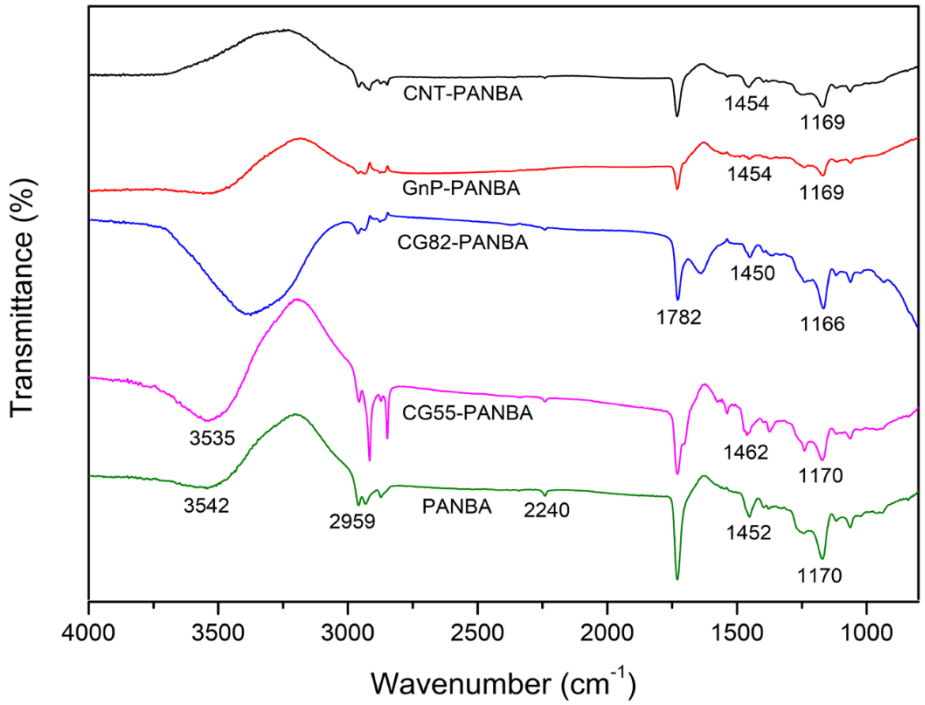

Figure 7. FT-IR spectra of PANBA and composite hybrid binders.

Water-emulsified polymer binders require the dispersion stability for a certain period suggested by customers. Destabilized dispersion caused by creaming, sedimentation, and coalescence makes a serious problem during the slurry making process, resulting in a failure in the slurry coating into current collector. The TSI value computed from backscattering and transmission signals describes such destabilization phenomena quantitatively; higher values reflect more instability. As shown in Figure 8, the CNT- containing PANBA emulsified solutions are more stable than the GnP-PANBA solution. It is one of the advantages to employ CNT as a conductive nanofiller of PANBA emulsion as well as GnP. This must be due to better dispersion stability of the original CNT 1 wt% solution than the GnP 1 wt% solution. The GnP solution had a small amount of aggregated domains after the dispersion using ultrasonication, whereas CNT aggregates were barely observed in the CNT solution.

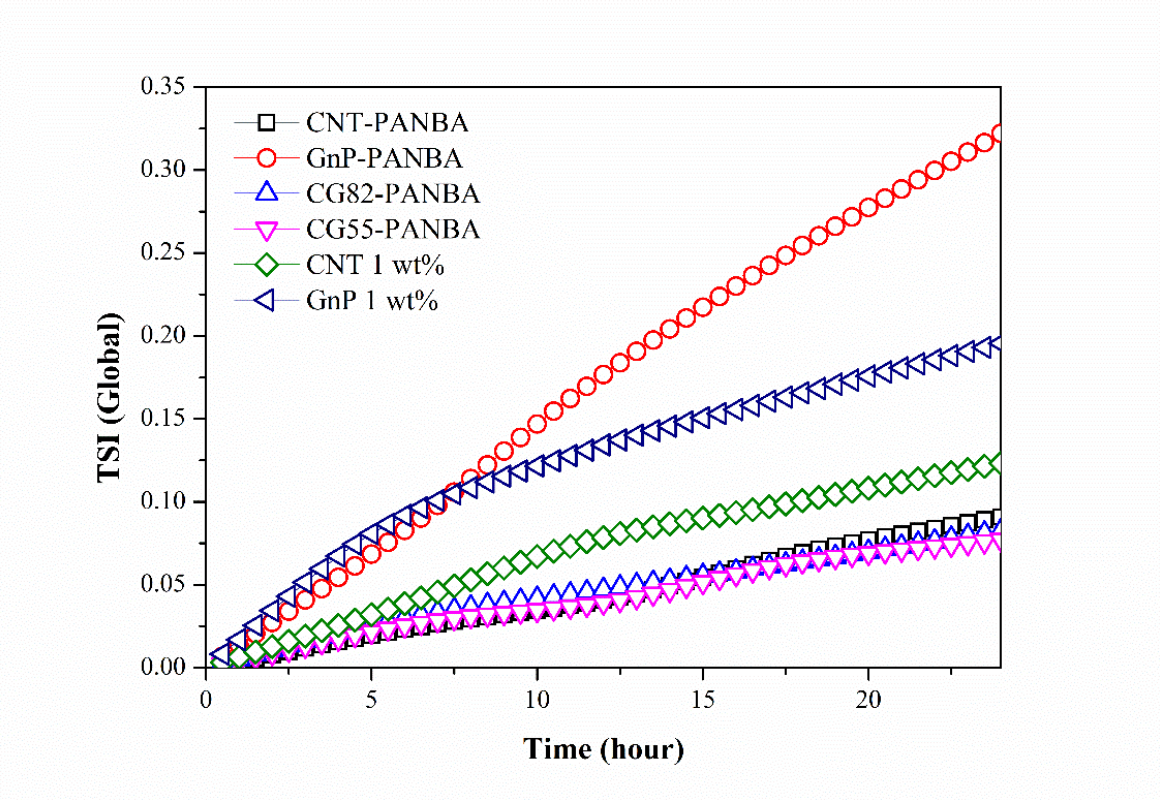

Figure 8. Turbiscan dispersion stability of the CNT-, GnP-, and CNT-GnP hybrid-PANBA emulsions including the GnP and CNT solutions.

Main objectives to use the conductive nanofillers in the emulsified PANBA binder are to improve electrical conductivity and mechanical properties by constructing overlapped structures of either GnP or CNT in binder. The sheet resistance (R_{sh}) of the binder films are first measured and listed in Table 3. As expected, the sheet resistance of a nonconductive PANBA film is out of range from the device. On the contrary, the conductive binder films have considerably low resistances. In particular, the hybrid samples show as low resistance as GnP-PANBA, whereas the CNT-PANBA has relatively higher resistance than the GnP-PANBA. Thus, even a small amount of graphene might construct layer-by-layer overlapping structures to help the increase in electron conduction.

Table 3. The Sheet resistance of binder films.

	PANBA	CNT-PANBA	GnP-PANBA	CG82-PANBA	CG55-PANBA
R_{sh} (Ω/□)	$>10^6$	3827.3	1794.5	1874.0	1866.8

The construct of layer-by-layers overlapping structure can be confirmed from the photos of binder films, which were taken after the applied elongation force of 50N to the films, in Figure 9. The CNT-PANBA couldn't stand the load and was broken, whereas no break occurred at the hybrid samples during the test. The sample containing relatively larger amount of CNT, CNT-PANBA and CG82-PANBA are harder to expand and contract than CG55-PANBA and GnP-PANBA. Additionally, the maximum strain of the GnP-PANBA was close to 7, whereas the CNT containing PANBA samples showed smaller strain values of approximately 4.

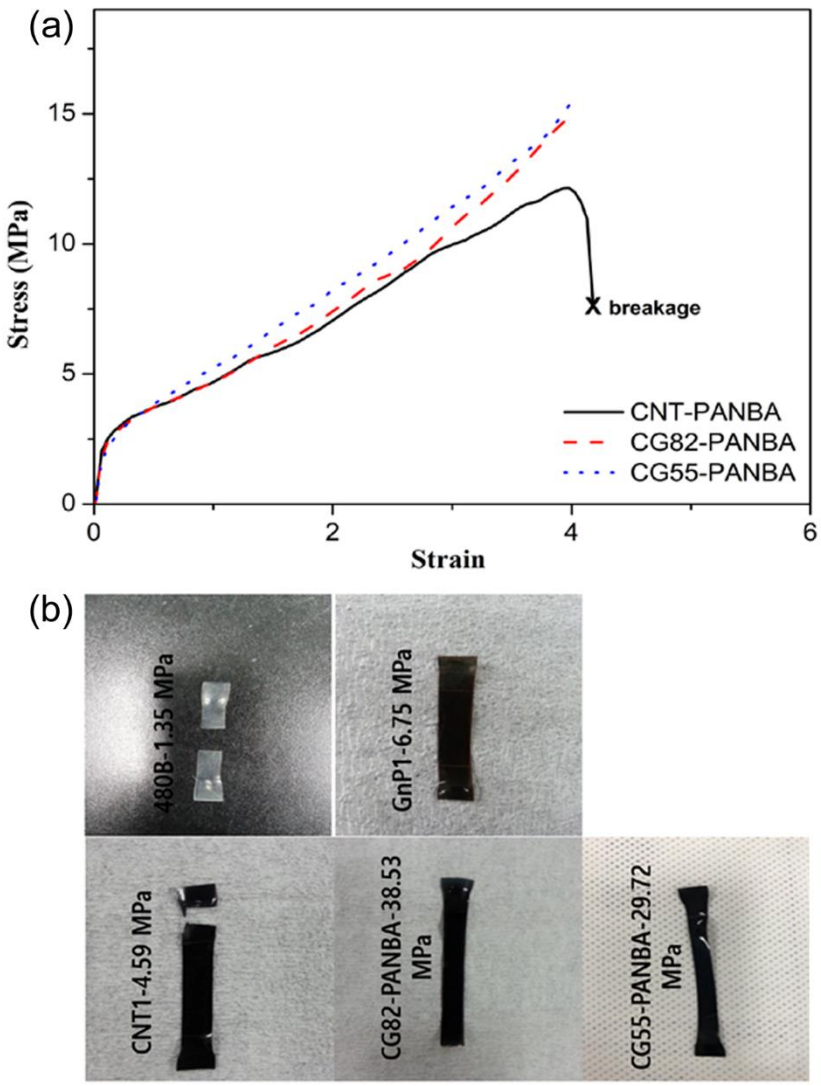

Figure 9. (a) Stress-strain profiles of the binder films with the propagation speed of 60 mm min-1, and the applied force of 50N (b) The elongation test of CNT-PANBA, GnP-PANBA and their combination binder of CG82-PANBA, CG55-PANBA with reference binder of 480B.

3.2 Application for electrode

3.2.1 $Li_4Ti_5O_{12}$ electrode

The electrochemical performance of the conductive emulsified binder, the electrodes composed of LTO active materials and the binders were galvanostatically charged and discharged for 100 cycles and the results are displayed in Fig 10(a). The conducting agent super-P was excluded from the LTO electrodes to clearly observe the effect of the conductive nanofillers in binder. Their performance was compared to the electrochemical performance of the LTO electrode containing the nonconductive PANBA binder. The LTO/PANBA electrode showed the lowest cyclic capacity of 118 mAh g^{-1} at the 100^{th} cycle, whereas the LTO electrodes composed of the conductive CNT-, GnP-, CG55- or CG82-PANBA binders showed better cyclic capacities above 130 mAh g^{-1} at the 100^{th} cycles, even though the differences are not meaningfully large. One of the drawbacks of high-powered LTO active materials is a significantly low electrical conductivity ($<10^6$ S cm^{-1})[28]. Even a much lower value of $\sim10^{13}$ S cm^{-1} was also reported through the four-point method[29]. This is noticeably lower than typical graphite electrodes ($\sim10^2$ S cm^{-1})[30]. Thus, the improvement in the electrical conductivity of emulsified binder contributes to the increase in the capacity of low conductive LTO electrodes. The electrical conductivity of the LTO material is considerably lower than that of typical graphite. The lack of the electrical conductivity of LTO leads to use a relatively large amount of conducting agent in its commercial application. The super-P 5wt% was used to the LTO electrodes fabricated for rate capability performance. The hybrid binder samples, CG55- and CG82-PANBA were chosen as representative conductive binders and compared with the nonconductive PANBA binder, because they possess several advantages simultaneously compared to the GnP- and CNT-PANBA binders: superior dispersion stability, and elongation, lower transport resistance for electron and ions, and lower charge transfer resistance. The result is shown in Fig 10(b). It is clear that such advantages of the hybrid conductive binders improved the rate capability of the LTO electrodes. Based on the reversible capacity at 0.2C, the LTO electrodes containing hybrid conductive binders maintain 55.1% and 29.5% at 5C and 10C for the CG55-PANBA, and 58.0% and 33.0% at 5C and 10C for the CG82-PANBA, respectively. However, the LTO electrode containing the nonconductive PANBA binder has only 44.1%

and 20.7% for 5C/0.2C and 10C/0.2C current ratios.

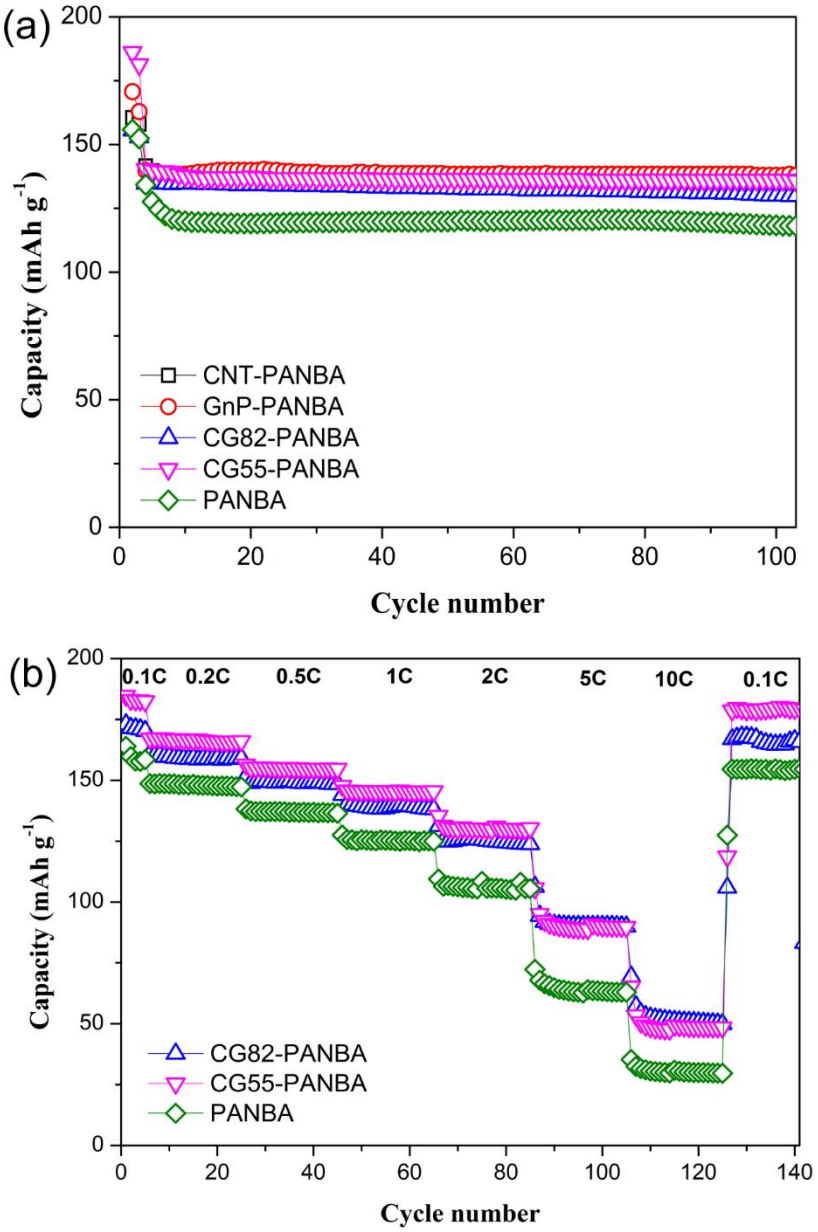

Figure 10. (a) Cyclic performance of the LTO electrodes containing only the conductive binders. Here no super-P conducting agent was added to the LTO electrodes (b) Rate capability test of LTO electrodes containing super-P as conducting agent.

The EIS analysis was also used to find out how the conductive binder affects the resistances related to electrode reactions, the ohmic resistance of solution, charge transfer resistance of the interfacial redox reaction, Warburg resistance of lithium ion, and so on. The impedance spectra of the LTO electrodes measured at 1.3V dc voltage before the charge/discharge cycle and after five cycles are depicted in Fig 11. The charge transfer resistance, represented by the size of semi-circles, of the fresh LTO/PANBA electrodes is compareable to those containing the conductive binders. This is not surprising because the impedance of the fresh electrode highly depends on the electrolyte wettability of the electrode as well as lithium and electron transport in the electrode. Nevertheless, the electrical conductivity shown in Table 2 must have an influence on lower charge transfer resistances of the grapheme-containing binder electrodes than the LTO/ CNT-PANBA electrode. The increase in cycle number generally decreases the charge transfer resistance due to the formation of more favorable environment for the mobility of lithium ions and electrons[31]. This can explain the decrease in the size of semi-circles in the five-cycled electrodes, compared to those in the fresh electrodes. Although the Warburg impedances are relatively low frequency invade the middle-frequency charge transfer impedance so thath the semi-circles are unclear, the charge transfer resistance of the cycled PANBA electrodes is large than those of the cycled LTO/conductive binder electrodes. Therefore, the conductive binder by CNT and GnP is also favorable to lowering the resistance for charge transfer kinetics at the electrochemically active interface. This must be achieved by the improvement in the transport of both electrons and lithium ions.

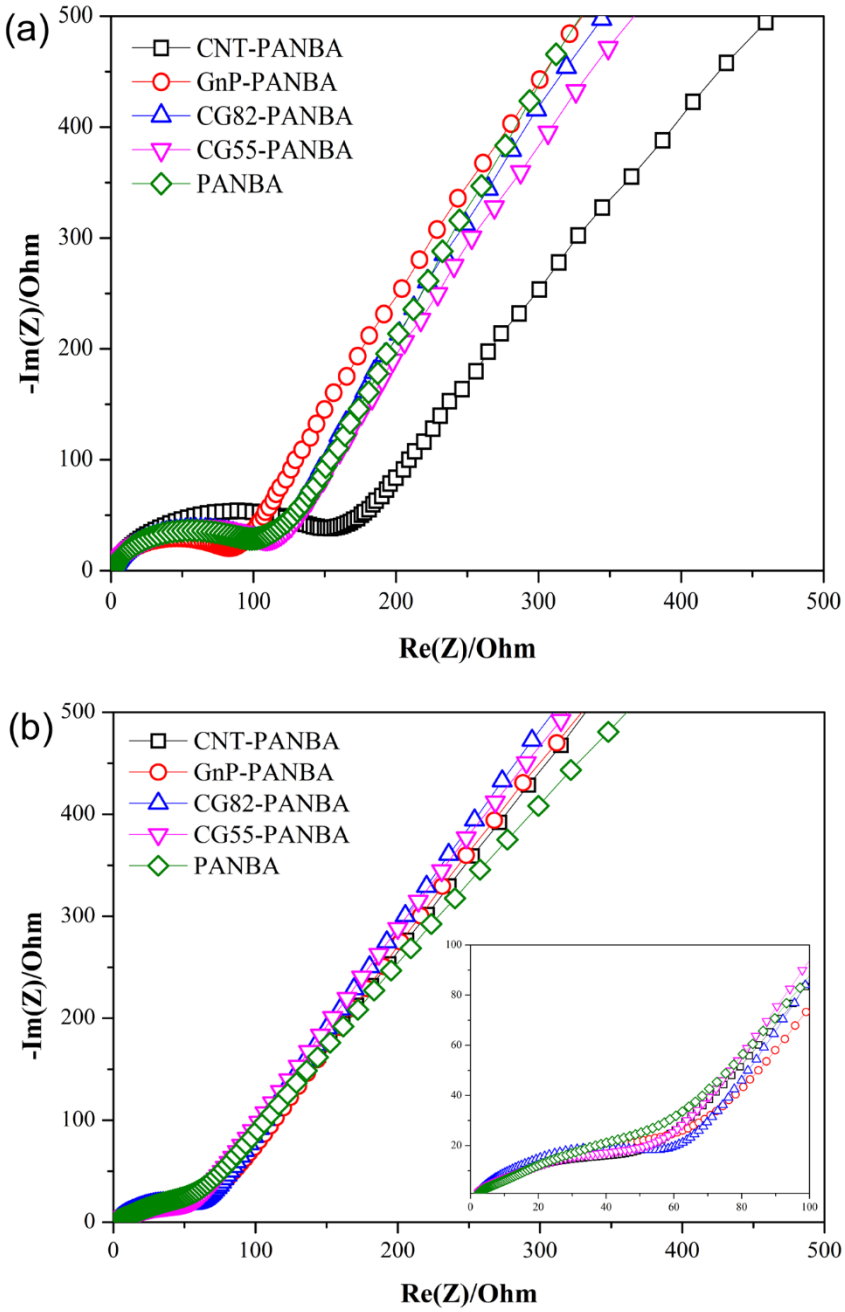

Figure 11. EIS of the LTO electrodes (a) before the charge/discharge cycle and (b) after five cycles.

To analyze the effect of the conductive binder on the electrochemical reaction of LTO, the CV of the LTO electrodes was first examined with various scan rates between 0.5 mV s^{-1} and 10mV s^{-1}. Two representative CV profiles at 1mV s^{-1} and 5mV s^{-1} are exhibited in Fig. 12. Regardless of the binder, the potential difference between anodic and cathodic peaks increases with increasing scan rates, indicating that the binder doesn't change the intrinsic quasi-reversible kinetics of the LTO redox reaction. However, it its easily seen that the relative increase in peak intensities by increasing the scan rate depends on the binder material. Additionally, the redox reaction occurs in a wide potential range with very sluggish redox peaks at 5 mV s^{-1}. Thus, the quasi-reversible kinetics is greatly dependent upon the diffusion of lithium ions, which is affected by the binder material. A linear relation between the peak current and the square root of scan rate was first solver using a convolution theorem by Randles[32] and Sevcik[33]. It is written for a quasi-reversible kinetics at room temperature as[34]

$$i_p = 2.65 \times 10^5 n^{3/2} C_{Li} A D_{Li}^{1/2} v^{1/2}$$

where i_p, n, C_{Li}, v, A, and D_{Li} are peak current in amperes, number of electrons transferred in the redox reaction, bulk concentration in mol cm^{-3}, scan rate in V s^{-1}, electrode area in cm^2, and diffusion coefficient in cm^2 s^{-1}, respectively. The diffusion coefficients are calculated from the slope of i_p vs. $v^{1/2}$ for both anodic and cathodic scans and listed in Table 4. Compared to the nonconductive LTO/PANBA electrode, the LTO electrodes containing the conductive binders showed better lithium, ion transport. This is attributed to the functional –COOH and –OH groups formed on the surface of CNT and GnP for their water dispersion. Jia et al[35] reported that functionalized CNTs embedded in a poly(ether ether ketone) provided enriched proton transport through its nanosheet and thus was inferior to the 1D turbular structure of CNT. This might explain why the LTO/CNT-PANBA electrode had higher diffusion coefficient than the LTO/GnP-PANBA electrode. The diffusion coefficients of the LTO electrodes composed of hybrid binder systems are as good as that of the CNT-PANBA electrode.

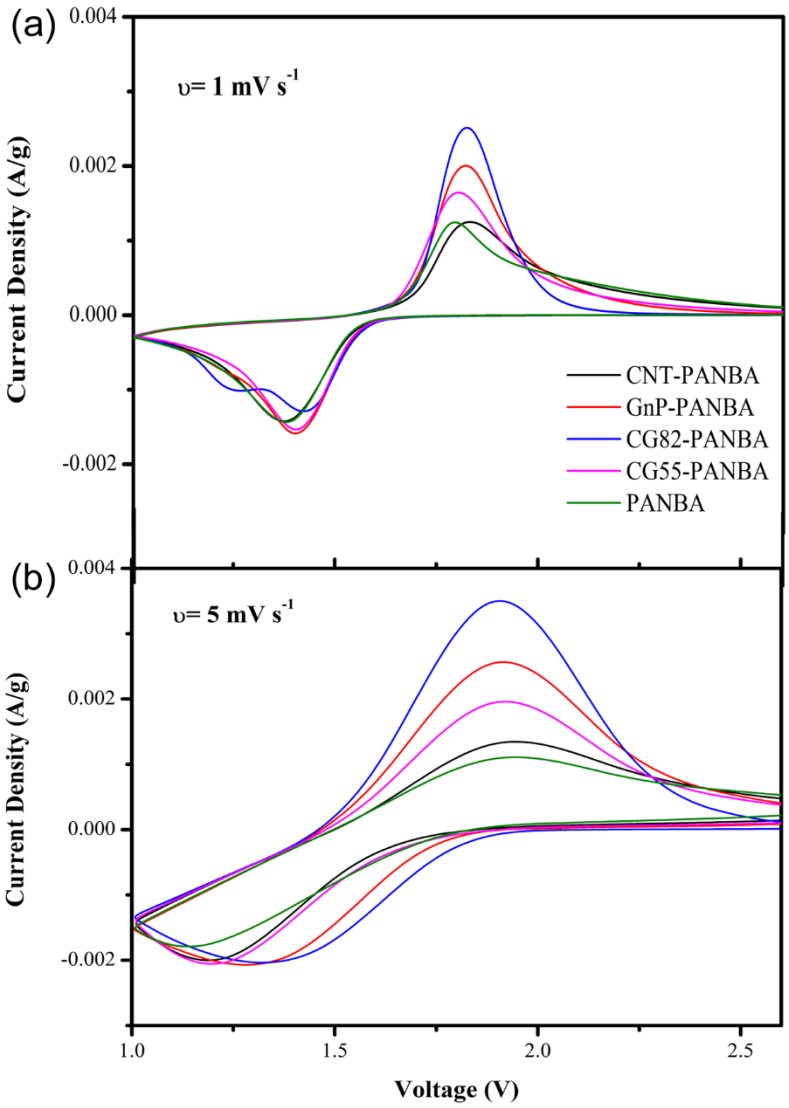

Figure 12. Cyclic Voltammetry profiles of the LTO electrodes measured (a) at 1 mV s^{-1}(b) at 5mV s^{-1}

Table 4. Lithium ion diffusion coefficients of the LTO electrodes calculated from the Randles-Sevcik equation.

Diffusion Coefficient ($cm^2\ s^{-1}$)	PANBA	CNT-PANBA	GnP-PANBA	CG82-PANBA	CG55-PANBA
Anodic process	4.98E-10	1.11E-08	3.36E-09	1.64E-08	1.12E-08
Cathodic process	5.54E-10	1.17E-08	9.39E-10	1.97E-08	1.24E-08

3.2.2 Graphite electrode

Diverse characterization techniques were used to analyze the results of the electrochemical performance of the graphite electrodes according to composite binders. In general, a binder affects the LIB performance by its adhesion capability, electrical resistance, and the transportation ability of lithium ions in an electrodes. All of CNT- and GnP-, and their composite binders are indistinguishable insulating polymers with an high electrical resistance. To investigate the adhesion capability of the nanofiller binders, 180˚peeling experiment of the graphite electrodes were performed, and the results are shown in Fig.13 (a). As we explained in the Fig 9 (b), that GnP fillers reinforced in the PANBA/GnP binders improved the mechanical elongation properties of the binder system, therefore, its contributing to the increase in their adhesion strength. In contrast, increasing of the amount of GnP in combination binders of CG82- and CG55-PANBA slightly increased the adhesion strength. The adhesive functional groups of the PANBA by their chemical bonds with proper amount of GnP ultimately leading to increase the adhesive property. Nevertheless, compared with the commercial 480B containing electrodes, the GnP-PANBA[12,36] and their composite binders CG82-, CG55-PANBA binders have higher adhesion strengths, which benefits the performance of a binder. In addition to the distribution of binders, the extent of the eletrolyte uptake of graphite electrode also affects the both lithium-ion mobility and edhesion in an electrode. An appropriate electrolyte uptake facilitates lithium-ion transport through the binder with not much change in the morphology including the crystallinity of binder. An excess uptake severely weakens the adhesion by changing the binder morphology and can cause the ultimate failure of the mechanical integrity of electrodes. Although GnP-PANBA, CG82-PANBA, and CG55-PANBA used electrodes uptake electrolyte to a small extent in the range of 10-13 wt% for 30 mins, as plotted in Fig. 13 (b). This indicates that no severe weakening in adhesion occurred when the electrodes were to exposed to electrolyte. We can clearly see that in cycle and rate capability test of graphite electrodes. Compared to these binders CNT-PANBA binder absorbed relatively smaller amount of electrolyte, however didn’t show better results in cycle and rate capability test.

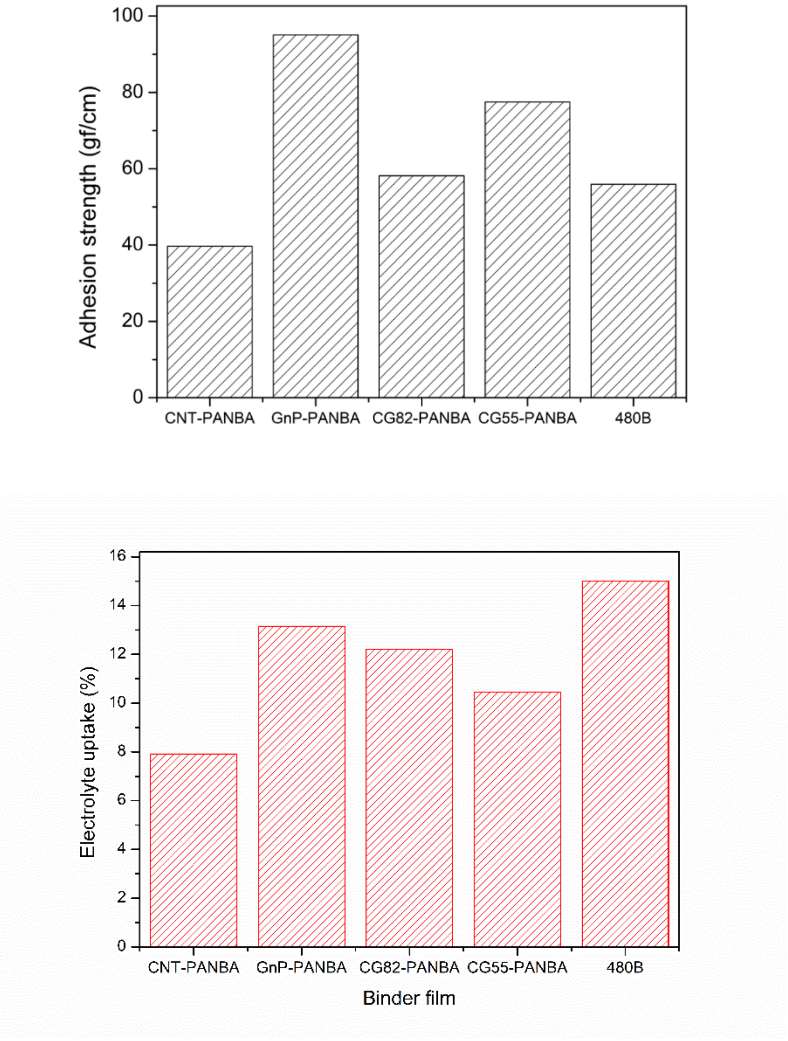

Figure 13. (a) Adhesion strength of graphite electrode (b) electrolyte uptake results of graphite electrode

The cyclic performances of the graphite electrodes using the CNT-PANBA, GnP-PANBA and their composites CG82-PANBA, CG55-PANBA binders are shown in Fig. 14(a). In these cases, the role of the conductive binders was not too dominant, as compared with commercial 480B reference. This is understandable because that graphite is a very good electrical conductive material and experiences a small volumetric change during cycles, so the addition of small amount of nanofillers to conductive binder to improve its mechanical and electrical properties cannot cause a great improvement in the cell performance. Even though conductive polymer binders show smaller capacity than commercial binder of 480B, the composite polymer binders of CG82-, CG55- and GnP-PANBA containing graphite electrode show higher reversible capacities than the CNT-PANBA electrode because we think graphene can provide more active sites for lithium ion absorption. Therefore, even though small amount of graphene and carbon nanotube can be increase the electrical performance of graphite electrode. As we can see slightly decrease of capacity during 100 cycle can be explained by volume expansion during the charge and discharge process. For graphite electrode, it suffers from volume expansion for 10%.

A very similar result was obtained from the rate capability tests, except that the graphite electrode containing commercial 480B shows a slightly higher capacity than that containing conductive nanofiller binder CNT-, GnP-, CG82- and CG55-PANBA as shown in Fig 14(b). At a low current rate of charge/discharge, there is not much difference in reversible capacity among the graphite electrodes. However, the difference is clearly seen with an increasing current rate. Meanwhile, the capacities of the electrodes are completely restored to their initial capacities when the rate returns to 0.1C from high-rate cycles. During all current rate, composite binder of CNT and GnP which is CG82- and CG55-PANBA binders shown higher capacities among conductive nanofiller binders of CNT- and GnP-PANBA binders. Therefore we can clearly see that composite nanofiller binders also can show better electrical conductivity for graphite electrode for LIB.

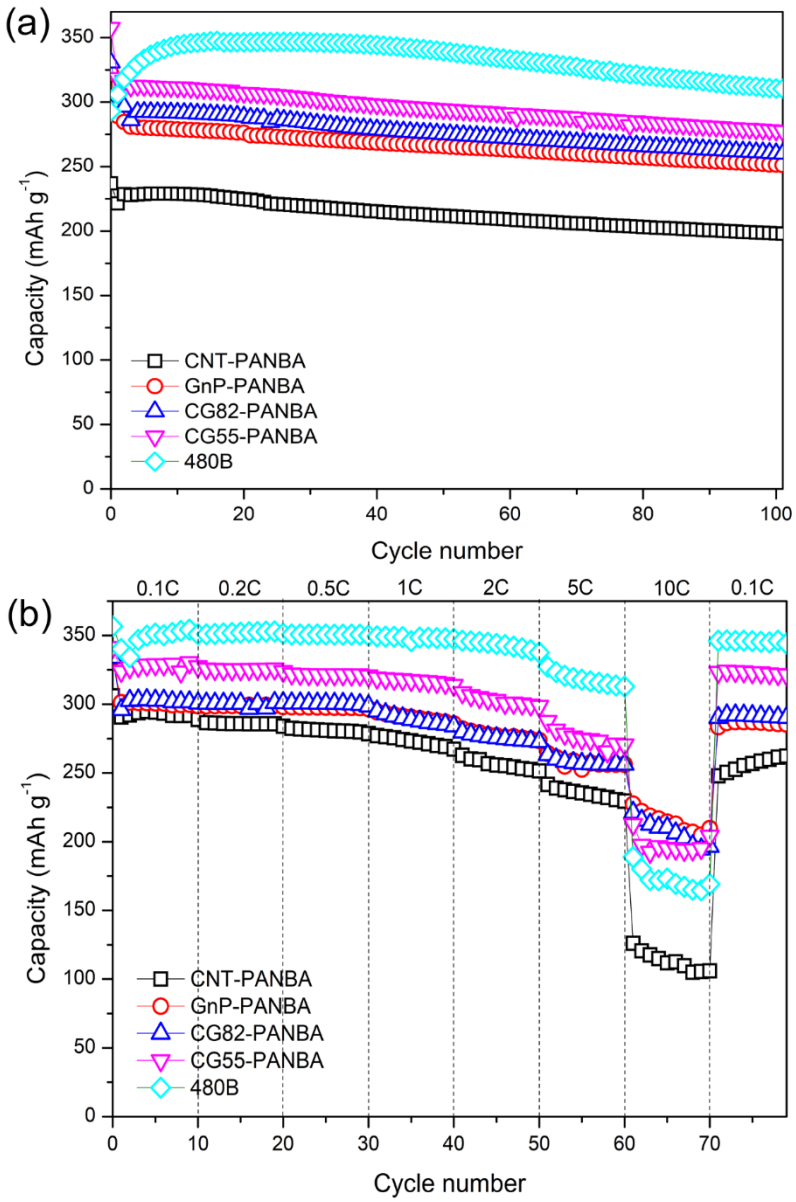

Figure 14. (a) Cyclic performance of the graphite electrodes containing conductive binders. (b) Rate capability test of graphite electrodes containing conducting agent of VGCF.

To examine the electrochemical stability of the nonconductive PANBA polymer with conductive nanofillers of CNT-, GnP-, CG82- and CG55-PANBA samples with commercial 480B, the CV of the graphite electrodes was first examined with various scan rates between 0.5 mV s^{-1} and 10 mV s^{-1}. Two of representative CV profiles at 1 mV s^{-1} and 5 mV s^{-1} are exhibited in Fig 15 (a) and (b) respectively. CVs show the measured current divided by the weight of each the electrode. The cathodic and anodic peaks around 0V in Fig.16 are attributed to reversible intercalation/deintercalation reactions of lithium ions into/out of layered graphene nanoplatelet structure. Commercial binder of 480B current density is smaller than others with conducting nanofiller binders. Current density reveals that how the electrochemical reaction happens in the cell. As we seen from the sheet resistance in table 3, CNT nanofiller has higher electrical resistance than others. As we can see that increasing of scan rate the reduction peak shifted to right side. Due to the dispersion properties, the combination binder of CG82- and CG55-PANBA may not be as good as the only CNT- and GnP-PANBA binder. Therefore, it can be explained that conductive binders used for graphite electrode enhancing the electrical contact.

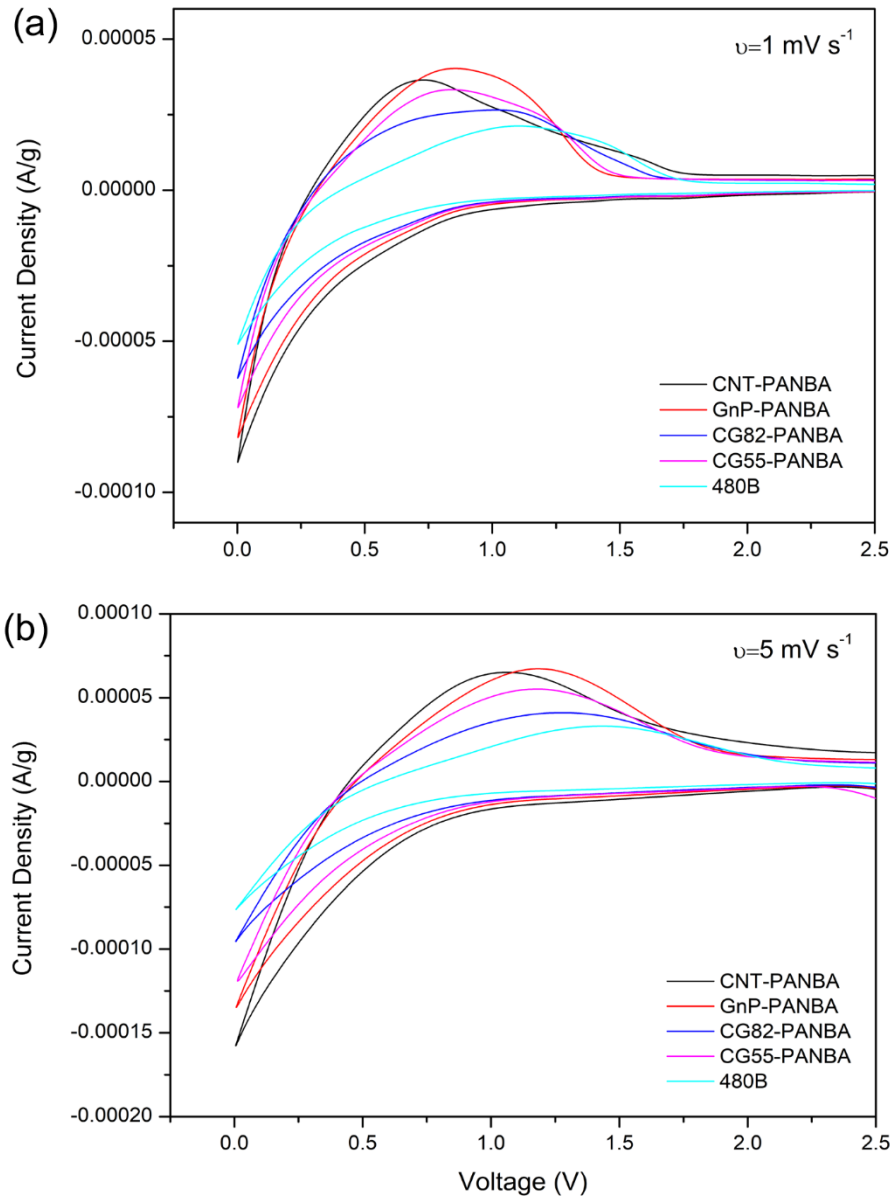

Figure 16. CV profiles of the graphite electrodes measured at the scan rates of (a) 1 mV s^{-1} (b) 5 mV s^{-1}

4. Conclusion

New water-dispersed nanocomposite binders composed of conductive CNT and GnP hybrid 1 wt% versus PANBA were successfully synthesized via an emulsion polymerization. The ratios of CNT to GnP in the nanocomposites were 0.8:0.2 and 0.5:0.5, respectively. The hybrid CG55- and CG82-PANBA samples show better water dispersion stability than the GnP-PANBA. They also have lower electrical resistances and higher tensile strength than the CNT-PANBA. Compared to the nonconductive PANBA-containing LTO electrode, the electrodes containing the conductive CNT-, GnP-, CG55-, or CG82-PANBA binders show better lithium ion diffusion because the functional groups formed on the surface of CNT and GnP provide enriched lithium ion transport pathways. Due to the favorable 1D turbular structure of CNT for lithium ion transport, the LTO/CG55-PANBA and LTO/CG82-PANBA electrodes have higher diffusion coefficients than the LTO/GnP-PANBA electrode. Such advantages of the CG55- and CG82-PANBA binders improve the electrochemical performance of the LTO electrode.

In graphite electrode case, all the hybrid conductive binders compared with high conductive reference binder of 480B. In this case, CNT-, GnP-, CG55- and CG82-PANBA binders show lower capacity than reference binders, however combined hybrid binders such as CG55- and CG82-PANBA binders show higher specific capacity than conductive CNT- and GnP-PANBA binders. Therefore we can say that combination of this two conductive nanofillers can show better results to anode materials of lithium ion battery.

5. Reference

1. R. Van Noorden, *Nat. News*, **507**, 26 (2014).

2. B. Scrosati and J. Garche, *J. Power Sources*, **195**, 2419–2430 (2010).

3. M. Armand and J.-M. Tarascon, *Nature*, **451**, 652–657 (2008).

4. J. Chong et al., *J. Power Sources*, **196**, 7707–7714 (2011).

5. C. de las Casas and W. Li, *J. Power Sources*, **208**, 74–85 (2012).

6. X. Wang, Y. Hou, Y. Zhu, Y. Wu, and R. Holze, *Sci. Rep.*, **3**, 1401 (2013).

7. M. Nie, D. P. Abraham, Y. Chen, A. Bose, and B. L. Lucht, *J. Phys. Chem. C*, **117**, 13403–13412 (2013).

8. M. S. Whittingham, *Chem. Rev.*, **104**, 4271–4302 (2004).

9. M. Winter, J. O. Besenhard, M. E. Spahr, and P. Novák, *Adv. Mater.*, **10**, 725–763 (1998).

10. F.-C. Chiu, Y.-C. Chuang, S.-J. Liao, and Y.-H. Chang, *Polym. Test.*, **65**, 197–205 (2018).

11. M. Yoo, C. W. Frank, S. Mori, and S. Yamaguchi, *Polymer*, **44**, 4197–4204 (2003).

12. M. H. T. Nguyen and E.-S. Oh, *Electrochem. Commun.*, **35**, 45–48 (2013).

13. J.-H. Lee, S. Lee, U. Paik, and Y.-M. Choi, *J. Power Sources*, **147**, 249–255 (2005).

14. R. Wang et al., *Nanoscale Res. Lett.*, **12** (2017) https://www.ncbi.nlm.nih.gov/pmc/articles/PMC5662525/.

15. J. Drofenik et al., *Electrochimica Acta*, **48**, 883–889 (2003).

16. L.-H. Huang, D. Chen, C.-C. Li, Y.-L. Chang, and J.-T. Lee, *J. Electrochem. Soc.*, **165**, A2239–A2246 (2018).

17. S. Komaba et al., *J. Power Sources*, **195**, 6069–6074 (2010).

18. L. Gong, M. H. T. Nguyen, and E.-S. Oh, *Electrochem. Commun.*, **29**, 45–47 (2013).

19. M. Yoo, C. W. Frank, and S. Mori, *Chem. Mater.*, **15**, 850–861 (2003).

20. S. S. Zhang, K. Xu, and T. R. Jow, *J. Power Sources*, **138**, 226–231 (2004).

21. J. Song et al., *Adv. Funct. Mater.*, **24**, 5904–5910 (2014).

22. F. Bigoni, F. D. Giorgio, F. Soavi, and C. Arbizzani, *J. Electrochem. Soc.*, **164**, A6171–A6177 (2017).

23. F. M. Courtel, S. Niketic, D. Duguay, Y. Abu-Lebdeh, and I. J. Davidson, *J. Power Sources*, **196**, 2128–2134 (2011).

24. S.-J. Kim, B.-R. Lee, and E.-S. Oh, *J. Power Sources*, **273**, 608–612 (2015).

25. B.-R. Lee and E.-S. Oh, *J. Phys. Chem. C*, **117**, 4404–4409 (2013).

26. C. Lin et al., *J. Mater. Chem. A*, **2**, 9982–9993 (2014).

27. H. Mittal et al., *Carbohydr. Polym.*, **98**, 397–404 (2013).

28. X. Li, M. Qu, and Z. Yu, *J. Alloys Compd.*, **487**, L12–L17 (2009).

29. C. H. Chen et al., *J. Electrochem. Soc.*, **148**, A102–A104 (2001).

30. I. M. Dougall, *Handbook of Ferroalloys: Chapter 4. Ferroalloys Processing Equipment*, p. 100, Butterworth-Heinemann, (2013).

31. http://www.sciencedirect.com/science/article/pii/S0013468612003209.

32. J. E. B. Randles, *Trans. Faraday Soc.*, **44**, 327–338 (1948).

33. A. Ševčík, *Collect. Czechoslov. Chem. Commun.*, **13**, 349–377 (1948).

34. D. A. C. Brownson and C. E. Banks, *The Handbook of Graphene Electrochemistry*, Springer-Verlag, London, (2014) //www.springer.com/la/book/9781447164272.

35. S. Liu, X. Meng, J. Wang, and J. Xu, *High Perform. Polym.*, **29**, 602–607 (2017).

36. M. H. T. Nguyen and E.-S. Oh, *J. Electroanal. Chem.*, **739**, 111–114 (2015).